INTERNATIONAL JOURNAL OF
ENERGY AND ENVIRONMENT

Imam Al-Kadhum College (IKC) Conference on Applications of Engineering Techniques in Renewable Energy and Environment (AETREE), Najaf, Iraq, 5th May 2019.

Journal homepage: www.IJEE.IEEFoundation.org

The effect of annealing temperature on the structural and optical properties of nanostructure ZnO

Radhiyah M. S.al jarrah[1], Iman Muslim Alessa[2]

Department of Physics, Faculty of Science, University of Kufa, Najaf, Iraq.
[1] Email: rathyah@yahoo.com, [2] Emanmuslim8@gmail.com

Abstract
In this research, the effect of annealing temperature Ta on the structural and optical properties of ZnO nanostructure which was prepared by spray pyrolysis method, was investigated. ZnO films prepared by spray pyrolysis technique on glass substrate with thickness 300 nm using: Zinc acetate Zn $(CH_3COO)_2 \cdot 2H_2O$, with purity of 99.6% and distilled water. After that the films were annealed at various temperatures (673, 7 773 and 873 K). X-ray diffraction studies show that the structure of all ZnO films is polycrystalline with hexagonal wurtizte structure with preferential orientation in the (002) direction. The post-deposition annealing of the film from (R.T to 873) K increases the intensity of (002) peak corresponding to c-axis orientation in addition with the decrease in full width at half maxima (FWHM). The optical measurement showed that the nature of the optical transition has been direct allowed with average band gap energies have tendency to decreases from (3.28 -2.93) eV with increasing of Ta excepted it was increased to 3.21 eV at 773 K. The extent and nature of transmittance and optimized band gap of the material assure to utilize it for photovoltaic applications.
Copyright © 2019 International Energy and Environment Foundation - All rights reserved.

Keywords: Annealing; Band gap; Hexagonal wurtizte; Microstrain; Spray pyrolysis.

1. Introduction
In the last decade, the number of publications on ZnO has been increased annually and in 2007 ZnO had become the second most popular semiconductor after Si, and its popularity is still increasing with time [1-3]. ZnO has several favorable properties such as: good transparency, high electron mobility, wide and direct band gap, and strong luminescence [1, 2]. Therefore, it has gained substantial interest in the field of semiconductor research. Those properties already used in emerging applications for transparent electrodes in liquid crystal displays, energy-saving, heat-protecting windows, and electronic applications of ZnO as thin-film transistor and light-emitting diode, solar cell, sensors and detectors [3-6]. The purpose of this work is to finding the best temperature for creation of ZnO film and research of their figure of merits characteristics.

2. Experimental work
Nanostructure ZnO film was fabricated by spraying 0.1 M concentration of Zinc salt solution on glass substrate at temperature of 450 ^oC, The Zinc solution was prepared by solving 4.39 g of the Zinc acetate

dehydrate $Zn(CH_3COO)_2.2H_2O$ (molecular weight 219.4954 g/mole) in 100 mL of distilled water. The spray rate of the solution was adjusted to be one sprinkling in a minute and the sprinkling time was about 8 seconds. The normalized distance between the spray nozzle and the substrate was 27 cm. ZnO films were treated thermally at different temperatures, i.e., room temperature (RT), 673, 773 and 873 K for two hours in air. The structure of the films was examined by X-Ray Diffraction (XRD) using a Philips X-ray diffractometer system which records the intensity as a function of Bragg's angle. The source of radiation was Cu (kα) with wavelength λ=1.5406 oA, the current was 30 mA and the voltage was 40 kV. The scanning angle 2θ was varied in the range of 20°-60° and Atomic Force Microscope (AFM), (AA3000 Scanning Probe Microscope SPM, tip NSC35/AIBS) shown in photo plate 3.5 from Angstrom Advance Inc. tests were employed to examine the structure.
The optical properties of ZnO thin films deposited on glass slide which include the transmittance and absorbance spectra were studied over the wavelength range (200-1100) nm by using Shimadzu UV / Visible recorder spectrometer model 12600. During scanning, a blank glass slide was placed in one of the beam's direction and another glass slide with film deposit was in the other beam's direction. Thus, the absorption spectrum displayed by the UV/Visible spectrophotometer was as a result of the films deposited on the glass slide substrates. Mention the device(s) used in Optical Properties tests.
The absorption coefficient (α) which is a measure of the rate of light loss was calculated from absorption spectrum using this equation [7],

$$\alpha = 2.303\left(\tfrac{A}{t}\right) \tag{1}$$

The incident photon energy (E) determent using the following equation [8],

$$E(eV) = \frac{1240}{\lambda(nm)} \tag{2}$$

The optical energy gap determined using the Tauce equation [9],

$$(\alpha h\nu)^2 = B(h\nu - E_g) \tag{3}$$

where B is constant and E_g is the energy gap.
In polycrystalline semiconductors where there are localized states in their energy gaps, the absorption edge becomes wide. The width of these localized states can be calculated by using Urbach rule [10],

$$\alpha = \alpha_O \exp(h\nu / E_u) \tag{4}$$

where E_u is Urbach energy which is the width of the tails of the localized state in the forbidden band. Optical constants included refractive index (n), extinction coefficient (k) were calculated.

3. Results and discussion

3.1 X-ray diffraction analyses

Figure 1 shows XRD patterns. The structure of all ZnO films is polycrystalline with hexagonal wurtzite and preferential orientation in the c-axis at (002) direction. The highest peak can be observed at 2θ ~ 34.1°, which can be attribute to the plane (002) of the hexagonal ZnO. The other peaks at 2θ = 31.42°, 36.04, 47.44° and 56.33° is due to effect of (100), (101), (102) and (110) planes respectively [11]. Also, Figure 1 turns out that the annealing process improved the structure especially at (773 K) .
Since the total breadth of a XRD peak can be separated into contributions from the finite crystallite size and the presence of strain in the crystal, the plot has been used to determine the crystallite size and strain in the ZnO thin films using the formula [12]:

$$\beta \cos\theta = \frac{0.9\lambda}{G} + 4\varepsilon \sin\theta \tag{5}$$

 ©2019 International Energy & Environment Foundation. All rights reserved.

where λ = 1.54059Å, which is the wavelength of X-ray, G is the crystallite size, ε is the microstrain and β is the full width at half maximum at diffraction angle 2θ in radian. A straight line fit in the plot of Bcosθ and sinθ yields the values of crystallite size as well as microstrain as in Table 1. From the table we observed that the crystallite size is maximum when annealing temperature was 773 K, and further increase in the annealing temperature to 873 K, the crystallite size decreased. This may be due to the fact that on heat treatment which the flow of fluid near the substrate interface coagulates, to reorganize the grain size to increase. The coagulation process discontinues on further increasing the heat temperature with threshold around 773 K [13]. Furthermore, the microstrain value corresponding to the annealing temperature of 773 K was also maximum indicating the increased tensile strain in the crystallite of the film sample.

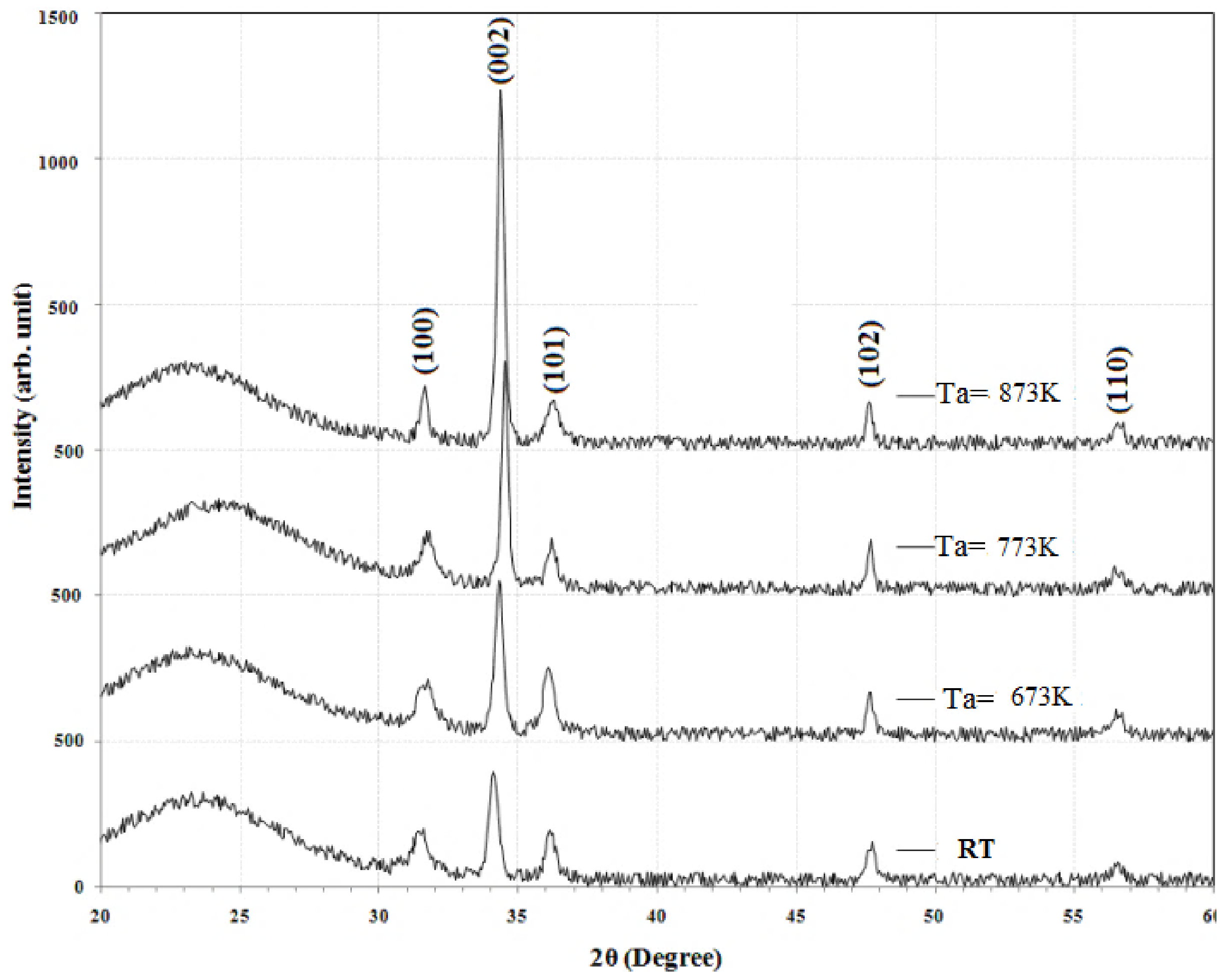

Figure 1. XRD spectrum of ZnO thin films with annealing temperatures.

Table 1. Crystallite size and microstrain values for ZnO films with annealing temperatures.

T_a (K)	2 θ (Degree)	G (nm)	ε × 10^{-4}
R.T	33.92	33	10
673	34.10	46	13
773	34.30	81	20
873	34.16	73	18

3.2 surface morphology

The surface morphology as in Figure 2, (a, b, c and d) are shown there are uniform distribution of homogeneous with spherical grains and an increasing in the grain size with annealing temperature. The average surface roughness, (RMS) values and the average surface grain size are listed in Table 2. This

ISSN 2076-2895 (Print), ISSN 2076-2909 (Online) ©2019 International Energy & Environment Foundation. All rights reserved.

result indicates that the growth of larger grains with increasing T_a leads to an increase in the surface roughness. The average grain size increases with increasing of Ta can be due to recrystallization in grains, leading to a reorientation of the film and a significant increase in average grain size.

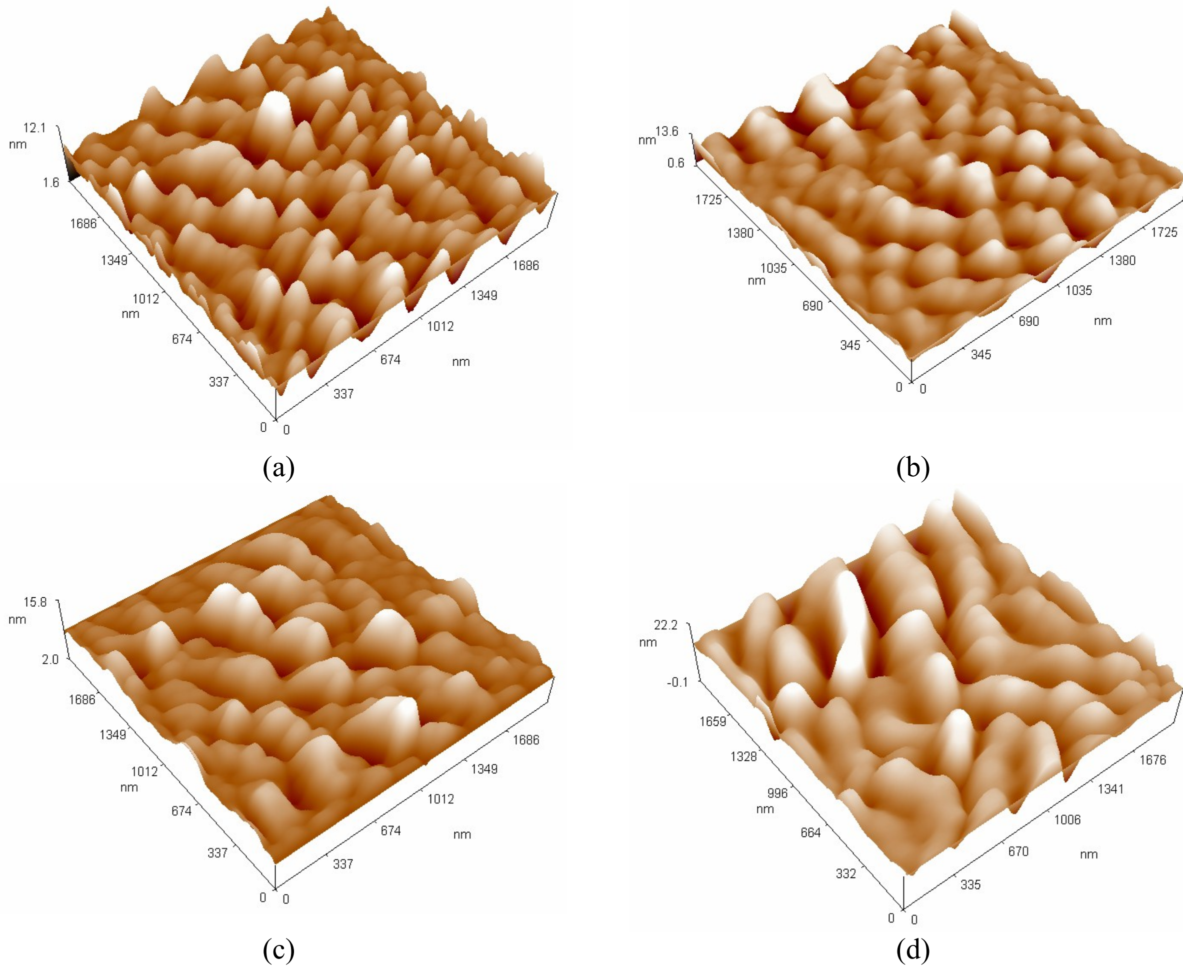

Figure 2. AFM images: (a) as deposited (b) annealed at 473 K, (c) 573 K and (d) 673 K.

Table 2. The average crystallite size and roughness average with T_a of ZnO thin films.

T_a (K)	Average crystallite size (nm)	Root mean square(nm)	Roughness average (nm)	Peak-peak (nm)
R.T	59.15	1.76	1.21	11.15
673	85.70	1.94	1.43	14.42
773	102.13	3.71	2.79	19.63
873	91.25	2.59	1.57	17.31

4. Optical properties

Figure 3 shows the transmission spectra of the ZnO films at different annealing temperatures. The spectra indicate smooth reflecting surface of the film and low scattering loss at the surface. The films annealed at (673 K and 873 K) exhibit a decreases in the transparency while at room temperature and film annealed at (773 K) exhibit good transparency in visible region (>70%).

The variation of refractive index n and extinction coefficient k with photon energy for ZnO films annealed at different temperatures are shown in Figure 4. As shown in the figures refractive index increases with increasing photon energy, with peak at about 3.1 eV. This can be attributed to the band gap. It may be noted that the refractive index n is almost unaffected by the variation in the annealing temperature up to the peak, after which it shows a small dependence on the annealing temperature [14].

ISSN 2076-2895 (Print), ISSN 2076-2909 (Online) ©2019 International Energy & Environment Foundation. All rights reserved.

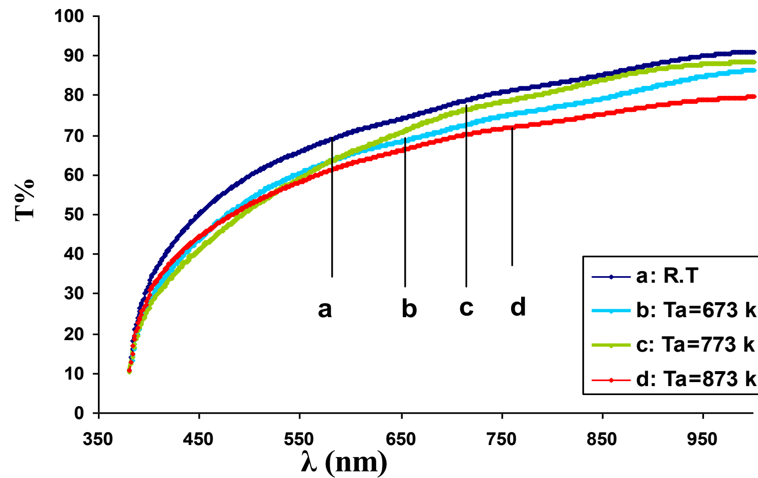

Figure 3. Transmittance spectrum as a function of λ for ZnO film at different annealing temperatures.

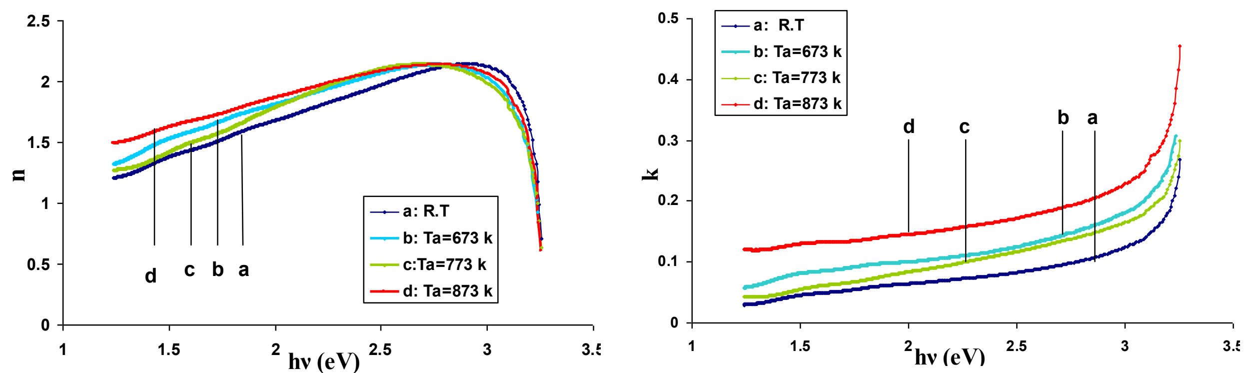

Figure 4. Variation of n and k with photon energy for thin ZnO film at different annealing temperatures.

For direct allowed transitions and it is known that ZnO is a direct band gap semiconductor. The variation of (αhν)2 vs. hν is shown in Figure 5. The energy gap E_g of the samples was evaluated from the intercept of the linear portion of each curve with the hν. Table 3 gives values of E_g with different annealing temperatures. From the figure clearly the band gap decreases with annealing temperature while it was increase at (773 K).

It is assumed that the absorption coefficient α near the band edge shows an exponential dependence on photon energy for many materials. This dependence is given by equation (4). The plot of lnα vs. photon energy hν for ZnO thin films annealed at (673, 773and 873 K) is shown in Figure 6 and E_u can be found from the slope.

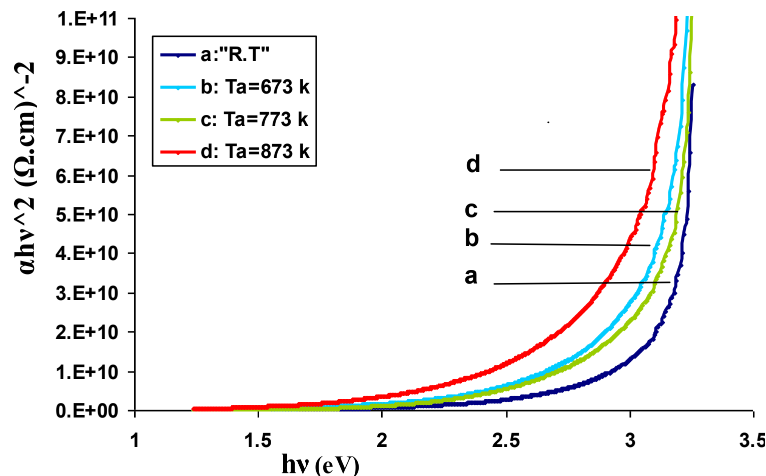

Figure 5. Variation $(\alpha h\upsilon)^2$ versus hυ for ZnO films at different annealing temperatures.

 ©2019 International Energy & Environment Foundation. All rights reserved.

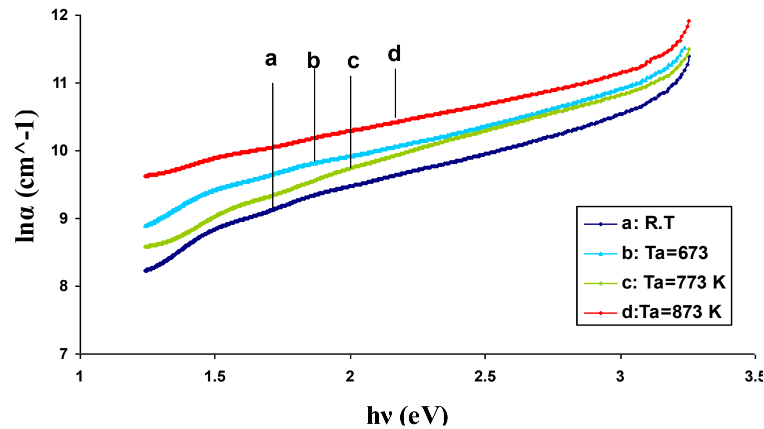

Figure 6. The variation of (ln α) versus hυ for ZnO thin films at different annealing temperatures.

Table 3. Optical parameters of ZnO films with different annealing temperatures.

T_a (K)	E_g (eV)	E_u (eV)
R.T	3.28	0.0815702
673	3.10	0.0962408
773	3.21	0.0762218
973	2.93	0.1206151

5. Conclusion

From the above this study it can be concluded that the temperature 773 K is the best for energy gap and crystalline size as well as the Urbach tail. Red shift of optical band gap with annealing temperature have been observed and from the band gap it was found that the ZnO films were emitting in Ultra violet region.

References

[1] Chennupati, Jagadish, & Stephen J. Pearton, Zinc oxide Bulk, Thin Films and Nanostructures, China: Elsevier. 2007.
[2] Nanda Shakti, P.S.Gupta, Structural and photoluminescence of ZnO thin film and nanowire, Optoelectronic and Advanced Material - Rapid Communication, 4(5), 662, (2010).
[3] Marina Davydova, Alexandr Laposa, Jiri Smarhak, Alexander Kromka, Gas-sensing behavior of ZnO/diamond nanostructures Beilstein J. Nanotechnol, 9, 22–29, (2018).
[4] M.F.A. Alias, H.Kh. Alamy and R.M. Aljarrah, the role of thickness on the structural and electrical properties DC magnetron sputtering nanoZnOthin films, Journal of Electron Devices, Vol. 14, pp. 1178-1185, (2012).
[5] Y.Ohya, T. Niwa, T. Ban, Y. Takahashi, Jpn. J. Appl. Phys, 40, 297, (2001)
[6] Parmanand Sharma, Amita Gupta, J.Frank Owens, Akhisha Inoue, K.V Rao, J. Magn. Magn. Mater, 282, 115, (2004).
[7] Ming-Fu. Li, Modern Semiconductor Quantum Physics, Singapore: World Scientific (2001).
[8] O. Manasreh, "Semiconductor Heterojunctions and Nanostructures", McGraw-Hill, (2005).
[9] J.Taus, [Amorphous and Liquid Semiconductor] Plenums Press, New York and London ,271 pp. 99, (1974).
[10] F. Urbach, P hys. Rev., 92 (1953) 1324.
[11] JCPDS-International Centre for Diffraction Data. All rights resaved ,PCPD Fwin Vol.1.30, card no. 36-1451, N 1997.
[12] Rachana Gupta and Mukul Gupta, Phys.Rev. B, 72, 024202, (2005 .(
[13] T.Ghosh, S. Bandopadhyay, K.K Roy., A.K. Maiti, K. Goswami, Cryst. Res. Technol., 44, 879, (2009).
[14] M.F.A.Alias, R.M.Aljarrah, H.KH.Al-Lamy and K. A.W. Adem, Investigation the Effect of Thickness on the Structural and Optical Properties of Nano ZnO Films Prepared by d.c Magnetron Sputtering, International Journal of Application or Innovation in Engineering & Management, Volume 2, Issue 7, (2013).